Magneto-Hydrodynamic Numerical Study of DC Electromagnetic Pump for Liquid Metal

Ahmed Daoud[1] and Nedeltcho Kandev[1,*]
[1] : Institut de recherche d'Hydro-Quebec (LTE) Quebec, Canada
*Corresponding author: 600, Avenue de la Montagne, Shawinigan, (Québec), Canada, G9N 7N5,
kandev.nedeltcho@ireq.ca

Abstract: In this work, the results are presented of a 3D numerical magneto-hydrodynamic (MHD) simulation of direct current (DC) electromagnetic pump for liquid aluminum at large Reynolds number under externally imposed non-uniform magnetic field. The formulation of the magneto hydrodynamic model has been derived from the Reynolds-Averaged Navier-Stokes equations with standard k-ε turbulence model coupled with the Maxwell equations for Newtonian incompressible fluid. These equations are solved simultaneously in the finite element environment COMSOL 3.4a. A direct electrical current is applied to a pair of electrodes, placed orthogonally to the magnetic field, exerting the Lorentz force driving the molten metal through a flat rectangular channel. Several pumping operation conditions are applied to study the M deformations of the initial flow velocity profile in the magnetic field region.

Keywords: DC electromagnetic pump, MHD flow, finite element method.

1. Introduction

The electromagnetic pumping (EMP) of electrically conductive fluid is of growing interest for many industrial applications requiring precise flow control, enabling to break the flow or reverse flow direction without any moving parts or mechanical devices.

The concept of electromagnetic pumping was created first in the nineteen sixties where it was used in the nuclear industry to pump sodium. The pump concept for zinc and later for aluminum was developed in the nineteen seventies. Today, different EM pump systems are widely used in many metal melting environments such as extrusion billet casting, metal refinery for transporting molten metals, liquid metal circulation for alloys production etc. These pumps have many advantages over the mechanical pumps including precise flow control, reduced energy consumption and less dross formation.

In the DC electromagnetic pump, a direct electrical current is applied across a rectangular flat channel filled with electrically conducting fluid (molten metal) which is submitted to an orthogonal to the current permanent magnetic field. The interaction between the magnetic field and the DC current produces an electromagnetic Lorentz force driving the fluid through the flat channel.

The problem with the electromagnetic pumps is the non-homogeneous distribution of the fluid velocity profile and instability of the flow under certain operating conditions.

There are many numerical investigations and simulation results, concerning the MHD channel flows published over the last twenty years. I. J. Ramos and N. S. Winowich (1990) [1] applied finite element methodology to study MHD channel flow fields as a function of the Reynolds number, electrode length and the wall conductivity. It is shown that the axial velocity profile is distorted into M – shapes by the applied electromagnetic field and that the distortion increases as the Reynolds number and the electrode length are increased. M. Hughes and al. (1995) [4] used two-dimensional models under externally imposed permanent magnetic field to simulate the MHD flow in macroscopic scale and later, Suwon Cho (1998) [3] studied several analytical solutions using two-dimensional magnetic field analysis based on an equivalent current sheet model. These theoretical studies and numerical simulations predicted serious problems linked to the transformation of the velocity profile yielding the electromagnetic driving force in the opposite direction to the fluid motion especially at turbulent flow conditions.

In 1979 Richard J. Holroyd [9] presented the results of an experimental investigation of the flow of mercury along circular and rectangular non-conducting ducts in a non-uniform magnetic field at high Hartmann number. In this work, flow velocity, pressure and electric potential are

measured by hot-films probes. The author found that the flow in regions of non-uniform magnetic field is greatly disturbed but not in the dramatic manner predicted. In the recently appeared experimental investigation Andreev and al. [5] (2006), studied the liquid metal flow in rectangular duct under inhomogeneous magnetic field using the eutectic alloy GaInSn as the working fluid. In the experiments the Hartmann number was fixed at *Ha*=400 for the range of Reynolds number *Re* between 500 and 16000. Three regions of the flow development are identified in this investigation: a turbulence suppression region, a region with M-shape profile and a region with two wall jets.

In 2007, Votaykov E. V. and al. [7] investigated the structure of the three dimensional velocity field in a rectangular duct in fully developed laminar flow. For the numerical simulation the same geometry and magnetic field configuration as in the experiment of Andreev and al. [5] were used.

The majority of interesting MHD numerical investigations treated mainly laminar channel flow and they are not concerned with the DC pumping aspect. However, the question of simulation of turbulent MHD metal flow, involving braking and pumping aspect continued to remain open.

2. Physical principal and numerical method

The formulation of the magneto hydrodynamic model has been derived from the Reynolds-Averaged Navier-Stokes equations with standard k-ε turbulence model coupled with the Maxwell equations for Newtonian incompressible electrically conductive fluid. The governing equations can be summarized as follows:

$$\vec{J} = \sigma(-\nabla\varphi + \vec{v}\times\vec{B}) \quad (1)$$

$$\nabla.\vec{J} = 0 \quad (2)$$

$$\nabla.\vec{v} = 0 \quad (3)$$

$$\rho\frac{\partial\vec{v}}{\partial t} - \nabla.\left[\left(\eta + \rho\frac{C_\mu k^2}{\sigma_k\varepsilon}\right).\left(\nabla\vec{v} + (\nabla\vec{v})^T\right)\right] + \rho\vec{v}.\nabla\vec{v} = -\nabla P + (\vec{J}\times\vec{B}) \quad (4)$$

$$\rho\frac{\partial k}{\partial t} - \nabla.\left[\left(\eta + \frac{\eta_T}{\sigma_k}\right)\nabla k\right] + \rho\vec{v}.\nabla k = \frac{1}{2}\eta_T\left(\nabla\vec{v} + (\nabla\vec{v})^T\right)^2 - \rho\varepsilon \quad (5)$$

$$\rho\frac{\partial\varepsilon}{\partial t} - \nabla.\left[\left(\eta + \frac{\eta_T}{\sigma_\varepsilon}\right)\nabla\varepsilon\right] + \rho\vec{v}.\nabla\varepsilon = \frac{1}{2}C_{\varepsilon 1}\frac{\varepsilon}{k}\eta_T\left(\nabla\vec{v} + (\nabla\vec{v})^T\right)^2 - \rho C_{\varepsilon 2}\frac{\varepsilon^2}{k} \quad (6)$$

$$\eta_T = \rho C_\mu \frac{k^2}{\varepsilon} \quad (7)$$

Constant	Value
C_μ	0.09
$C_{\varepsilon 1}$	1.44
$C_{\varepsilon 2}$	1.92
σ_k	1.0
σ_ε	1.3

Here equation (1) is the Ohm's law, where φ is electric potential, *v* is the fluid velocity, ***B*** denote magnetic field density and σ is electrical conductivity of the fluid. The equation (2) represents the conservation of the electrical current, where *J* is the current density.

The fluid mechanics part of the problem is determined by equations (3), (4), (5) and (6) representing respectively the conservation of mass, momentum, turbulence kinetic energy (k) and dissipation rate (ε) of the fluid in motion. Equation (7) is used to calculate the kinematic eddy viscosity (η_T). The coupling between the electromagnetic model and the fluid one is done by introducing the Lorentz force $\vec{j}\times\vec{B}$ as a body force in the conservation of momentum (equation 4) and the use of the fluid velocity calculated by the fluid model in the Ohm's law (equation 1).

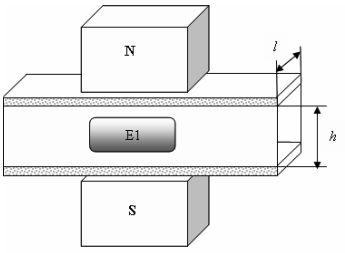

Figure 1. Simplified schema of the physical model of the electromagnetic DC pump used for the numerical simulation

The considered physical model of the electromagnetic pump is shown schematically in Figure 1. It consists on a rectangular flat channel of length *L* and height *h* with electrically insulated boundaries filled with molten metal with which is subjected to an externally imposed transversal magnetic field. A pair of electrodes E1 and E2 is introduced on the verticals

boundaries at right angle to the magnetic field to impose an electrostatic field E in the molten metal.

The Lorentz force F_{em} per unit mass, acting at a point of the considered domain is given by the cross product of the current density j and the magnetic field B in this point:

$$d\vec{F}_{em} = \vec{j} \times \vec{B} \qquad (8)$$

The total Lorentz pumping force in Newton, acting directly on the volume of the liquid metal, can be defined by integrating of all elemental forces dF_{em}.

It should be noted that the current density J has two components; the first component is due to the externally imposed electrostatic field $\vec{E}$, and the second one is due to the induced electromotive field $(\vec{v} \times \vec{B})$. In static conditions (without metal motion or in low laminar flow), the second term is zero or negligible and the Ohm'law is reduced to $\vec{J} = \sigma \vec{E}$ where E is the externally imposed electrostatic field. In this case the Lorentz pumping force can be defined as follows: $F_{em} = \sigma \vec{E} \times \vec{B}$.

In the case of turbulent flow under relatively large magnetic fields, a considerable increase in the hydraulic resistance is observed (Hartmann effect). This magneto-hydrodynamic effect is related to the fact that the vertical magnetic field generates a non-uniform negative horizontal electromagnetic force on the metal in motion which counteracts the velocity of the liquid metal by decreasing the thickness of the velocity boundary layers [3,6,8]. For a given channel geometry and magnetic field density B, this MHD phenomenon depends on the electrical conductivity σ, the density ρ and the viscosity of the liquid metal.

The induced electrical current is defined by the Ohm's law: $j_i = \sigma(\vec{v} \times \vec{B})$ and the negative electromagnetic force per unit mass will be $d\vec{F}_i = \vec{j}_i \times \vec{B}$

This magneto-hydrodynamic effect can be characterized by the Hartmann number, given by $Ha = B\,h\sqrt{\sigma / \mu}$, and by the interaction parameter $N = H_a^2 / R_e$, where, R_e is the Reynolds number $R_e = u_0 h / \nu$, and $\mu = \rho\nu$ is the dynamic and ν is the kinematic viscosities and u_0 is the mean velocity of the liquid metal.

3. Numerical modeling of the DC electromagnetic pump

The problem considered is described in section 2 and it is shown schematically in Figure 1. The externally imposed non-uniform magnetic field is simulated by introducing permanent magnets connected to an iron yoke on the top and bottom lateral walls of the rectangular channel. The relative permeability of the iron yoke is *murFe* = 4000, and the magnetization of the magnets is define as *Mpre* = 700000 (A/m). The magnetic and electric boundary conditions on external boundaries are: $\vec{n} \times \vec{A} = 0$ and $\vec{n}.\vec{J} = 0$, were A is the magnetic vector potential.

For this simulation, the liquid aluminum was used as electrically conductive fluid. It has density of 2385 kg/m^3, electric conductivity of 0.2 Ohm*m and kinematic viscosity of 0.545E-6 m^2/s . The Hartmann number is defined with half – height of the channel (h/2 = 0.001 m).

For the fluid model, the inlet and outlet boundary conditions of the rectangular channel are respectively P=P$_{inlet}$ and P=0 Pa. The inlet pressure P$_{inlet}$ was considered positive in the case of electromagnetic brake simulation and negative in the case of pumping. The negative value of pressure at the inlet is used to consider a pressure drop in the ducts before the channel. The remaining boundary conditions are taken as walls with logarithmic wall function.

In COMSOL 3.4a, three applications are used to carry out this simulation: k-ε turbulence model, conductive media DC and Magnetostatics.

After studying the mesh density effect on the simulation results, a meshing of 75165 elements was adopted. It generates some 980277 DOFs.

The simulations are carried out using a Double Quad Xeon (8 processors) workstation with 8Go of RAM. Using this computer we can carry out a simulation in approximately 5 hours.

4. Results of Simulation and Discussions

The simulations parameters and their global results are presented in the tables 1&2.

Table 1: Carried simulations

Case	Application	V_{el}	P_{inlet}
		[V]	[Pa]
1	Brake flow	0	8800
2	Pumping	0.05	-1000
3	Pumping	0.12	-350
4	Pumping	0.24	-5000

Table 2: Results of the carried simulations

Case	I	F_{total}	V_{inlet}	Re	Ha	N
	[A]	[N]	[m/s]			
1	0	-16.45	0.495	9081	434	21
2	498.5	3.78	0.517	9485	434	20
3	598.1	3.15	0.613	11246	434	17
4	1196.2	14.57	0.903	16567	434	11

The magnetic field density distribution on the straight line between the electrodes is shown in Figure 2. It can be seen in this figure that the maximum magnetic field of about 0.7 T is located at the lateral channel axis, while the magnetic field near the electrodes is 0.37 T.

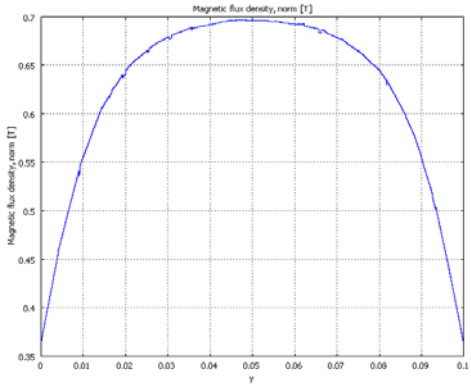

Figure 2. Magnetic field density on the straight line between the electrodes at z=0 and x=0.0025.

Figure 3. illustrates the magnetic field density distribution on the lateral *x* channel axis, where one can see again the maximum magnetic field density of 0.7 T on the center, between electrodes at x = 0.0025. For a given DC current I_{el} ,this magnetic field shape will determine the Lorentz force F_{em}, acting on the liquid metal.

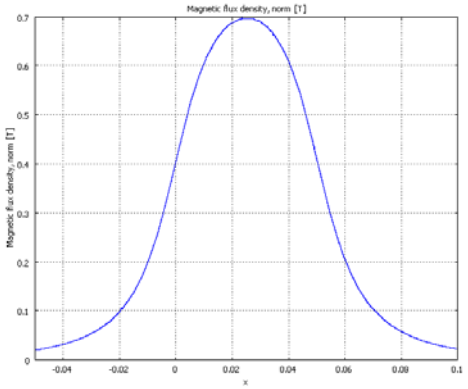

Figure 3. Magnetic field density on the lateral channel x axis at z=0 and y=0.

The total current density vectors distribution in the channel for the first case (brake flow) considered is illustrated in figure 3. In this case the imposed electrical potential between electrodes V_{el} is zero. There is induced electromotive field $(\vec{v} \times \vec{B})$ that is present around the region where the magnetic field is strong. This causes the induced current to flow in closed loops, as it can be seen in figure 4, and the system acts in the opposite to the flow direction as a brake.

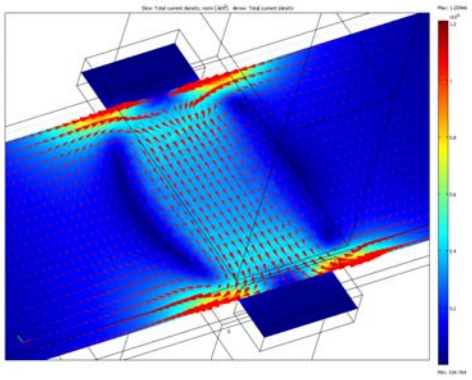

Figure 4. Total current density vectors distribution for the case 1 (brake flow)

Figure 5 shows a slice of the studied channel. Colors and arrows show the velocity magnitude along the channel in case1. We can notice four regions: A region of a constant velocity from the inlet until 1/3 of the channel, a region of braking beginning suddenly at the entrance of the region under the magnet and two regions of fluid

acceleration near the walls of the channel (called Hartmann layers (Votaykov E. V. and al. [7])) .

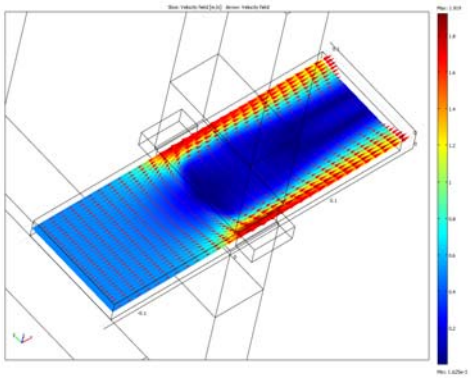

Figure 5. Velocity pattern along the studied channel (case 1)

Figure 6 shows the velocity profiles of the fluid at three positions of the channel (Inlet, middle and outlet) for the case1 (brake). At the inlet, the velocity is almost constant equal to 0.495 m/s. At the middle of the channel, the effect of Lorentz forces is at its maximum; an M-shaped profile can be noticed. In fact, the fluid decelerates and its velocity is almost equal to 0 m/s in the center while it accelerates (1.9 m/s) near the channel walls. Near the outlet, the fluid velocity profile still has the M-shaped form but we can notice that the velocity near the walls decreases (1.2 m/s) and a reverse flow at the center of the outlet appears. In this case, the total force applied on the fluid is -16.45 N.

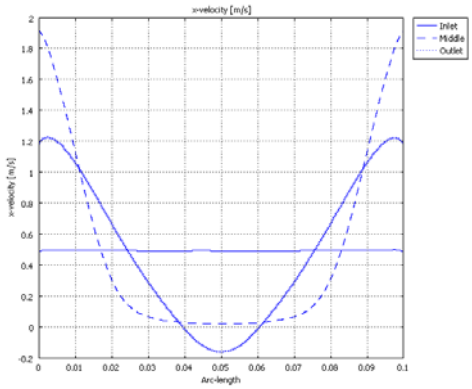

Figure 6. Velocity profiles in different positions of the channel (case 1)

In the case of electromagnetic pump (cases 2, 3 and 4), an externally imposed electrical field dominates over the induced electromotive field and the resulting electric current distribution produces in this case forces acting in such direction as a pumping system (see figure 7).

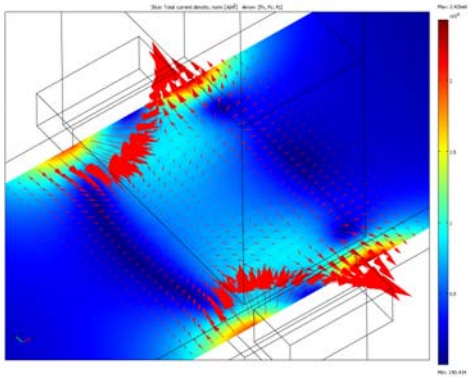

Figure 7. Lorentz force vectors and total current density distribution for the case 3 (pump)

Figure 8 shows a section of the studied channel. Colors and arrows show the velocity magnitude along it in case3. We can notice also four regions of interest like the brake case: A region of a constant velocity from the inlet until 1/3 of the channel, a region of low velocities beginning gradually at the entrance of the region under the magnet and two regions of fluid acceleration near the walls of the channel.

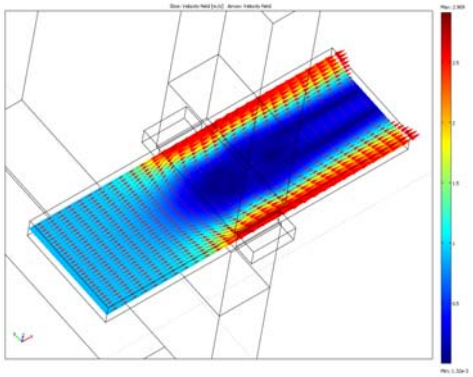

Figure 8. Velocity pattern along the studied channel (case 3)

Figure 9 shows the velocity profiles of the fluid at three position of the channel (Inlet, middle and outlet) for the case3 (pump). We can notice that the velocity profiles are almost

similar to the brake case. The velocity is at its maximum near the electrodes at the middle of the channel and near the walls (2.2 m/s). This acceleration induces an entrainment of the fluid at the inlet of the channel (0.613 m/s). The total force needed in this case for pumping is 3.15 N.

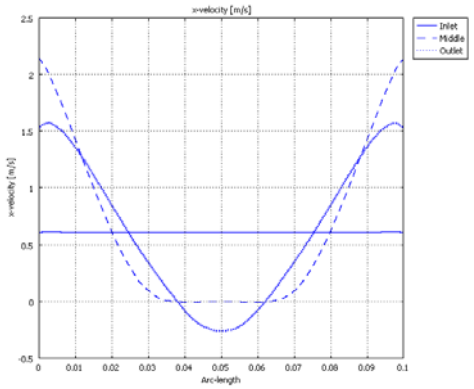

Figure 9. Velocity profiles in different positions of the channel (case 3)

5. Conclusions

In this paper, we presented the use of COMSOL 3.4a to simulate a 3D numerical magneto-hydrodynamic (MHD) direct current (DC) electromagnetic pump for liquid aluminum at large Reynolds number under externally imposed non-uniform magnetic field. Some numerical results of various cases (brake and pumping) were presented and discussed. Computations of the velocity field showed that all known general features (Hartmann layers and M shaped profile) are represented correctly by our numerical simulation. An experimental study of an MHD pump will be done to validate quantitatively the numerical results of the model.

6. References

1. Ramos I. J. and N. S. Winowich: Finite difference and finite element methods for MHD channel flows. *Int. J. Num. Methods* 11, PP. 907-934, 1990.
2. Lielausis O.: Development of ideas concerning the flow structure in inductive MHD pump channels, *Magneto-hydrodynamics*, Vol. 29, No. 4, 1993.
3. Suwon Cho and Sang Hee Hong: The magnetic field and performance calculations for an electromagnetic pump of a liquid metal: *J. Phys. D: Appl. Phys.* 31, PP. 2754-2759, 1998.
4. Hughes M., K. A. Pericleous and M. Cross: The Numerical modelling of DC electromagnetic pump and brake flow. *Appl. Math. Modelling*, Vol 19, PP. 713-723, Dec. 1995.
5. Andreev O., Yu Kolesnikov and A .Thess: Experimental study of liquid metal channel flow under the influence f a nonuniform magnetic field. *Phys Fluids, Vol 18, 065108*, 2006.
6. Gelfag A. Yu and P. Z. Bar-Yoseph.: The effect of an external magnetic field on oscillatory instability of convective flows in a rectangular cavity. *Physics of Fluids*, Vol. 13, No. 8, PP. 2269-2278, August 2001.
7. Votaykov Evgeny V., Egbert A. Zienicke: Numerical study of liquid metal flow in a rectangular duct under the influence of a heterogeneous magnetic field. *FDMP, vol.1,* pp 101- 117, 2007.
8. Mahmud S., S. H. Tasnim and M. H. Mamun: Thermodynamic analysis of mixed convection in a channel with transverse hydro-magnetic effect. *Int. J. of Thermal Sciences*, PP. 731-740, v. 42, 2003.
9. Richard J. Holroyd: An experimental study of the effects of wall conductivity, non-uniform magnetic field and variable-area ducts on liquid metal flow at high Hartmann number (Part 1: Ducts with non-conducting walls. *J. Fluid Mech, vol 93, part 4,* pp. 609-630, 1979.